ACS OMEGA

http://pubs.acs.org/journal/acsodf

Review

Mapping Spatiotemporal Heterogeneity in Tumor Profiles by Integrating High-Throughput Imaging and Omics Analysis

Pooja Annasaheb Patkulkar, Ayalur Raghu Subbalakshmi, Mohit Kumar Jolly,* and Sanhita Sinharay*

Cite This: *ACS Omega* 2023, 8, 6126−6138

Read Online

ACCESS | Metrics & More | Article Recommendations

ABSTRACT: Intratumoral heterogeneity associates with more aggressive disease progression and worse patient outcomes. Understanding the reasons enabling the emergence of such heterogeneity remains incomplete, which restricts our ability to manage it from a therapeutic perspective. Technological advancements such as high-throughput molecular imaging, single-cell omics, and spatial transcriptomics allow recording of patterns of spatiotemporal heterogeneity in a longitudinal manner, thus offering insights into the multiscale dynamics of its evolution. Here, we review the latest technological trends and biological insights from molecular diagnostics as well as spatial transcriptomics, both of which have witnessed burgeoning growth in the recent past in terms of mapping heterogeneity within tumor cell types as well as the stromal constitution. We also discuss ongoing challenges, indicating possible ways to integrate insights across these methods to have a systems-level spatiotemporal map of heterogeneity in each tumor and a more systematic investigation of the implications of heterogeneity for patient outcomes.

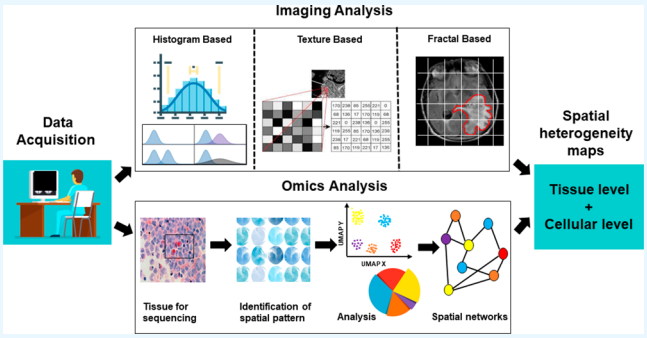

INTRODUCTION

The intrinsic heterogeneity in cancer cells can be attributed to their dynamic evolution in response to various stresses. This heterogeneity can manifest at many levels such as genomic, metabolomic, transcriptomic, epigenomic, and proteomic, exhibiting distinctly different molecular signatures. Clinical implications of this heterogeneity often result in inaccurate diagnoses hindering effective treatment and leading to worse outcomes across cancers.[1−4] Comprehensive molecular characterization of tumors through consortia such as The Cancer Genome Atlas (TCGA) Research Network have revealed specific subtypes in multiple cancers,[5,6] but recent investigations at a single-cell level have revealed that most, if not all, tumors contain cells from multiple subtypes, although in different proportions.[7−9]

Tumor heterogeneity does not have a singular cause; it accumulates from a multitude of factors such as genetic, transcriptomic, epigenetic, and microenvironmental variations. Intertumoral heterogeneity, which refers to heterogeneity in the same cancer between different patients, mainly originates from genetic and somatic alterations between patients, whereas intratumoral heterogeneity, which refers to heterogeneity in tumor cells within the same patient, originates from dynamic spatial and temporal variations in tumor cells or the tumor microenvironment within the same tumor.[4] This spatiotemporal variation in the tumor microenvironment causes tumors to have different resistance mechanisms in the same tumor, depending on the biopsied tumor's location.[10] This therapeutic resistance can be largely resolved by accurate analysis and mechanistic understanding of intratumoral heterogeneity. In this review, we discuss advances in emerging technologies such as high-throughput molecular imaging and spatial transcriptomics in assessing this intratumoral heterogeneity, to enhance the efficacy of personalized and adaptive cancer therapies.[11]

Molecular diagnostics with multiple advancements presently is unable to quantify all aspects of intratumor variability within an *in vivo* setting. For example, microarray analysis measures the transcriptome profiles in huge numbers of cells and provides an average measure of the bulk mass of cells/tissue, but it does not capture phenotypic and genotypic variance across cells, thus limiting its use for precision medicine. Spatial transcriptomic methods developed recently offer a better resolution for mapping intratumor heterogeneity by also classifying stromal signatures.[12]

Noninvasive molecular imaging methods of analyzing the whole tumor volume hold promise for clinical benefit through the characterization of morphological and functional signatures

Received: October 16, 2022
Accepted: January 5, 2023
Published: February 7, 2023

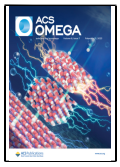

Downloaded via INDIAN INST OF SCIENCE on February 23, 2023 at 12:08:40 (UTC).
See https://pubs.acs.org/sharingguidelines for options on how to legitimately share published articles.

ACS Publications

© 2023 The Authors. Published by American Chemical Society

https://doi.org/10.1021/acsomega.2c06659
ACS Omega 2023, 8, 6126−6138

of intratumor heterogeneity.[13−15] Molecular imaging technologies such as computed tomography (CT), magnetic resonance imaging (MRI), positron emission tomography (PET), and particularly recent advances in image analysis methods have made appreciable headway toward exploring tumor heterogeneity. The significance of spatial structure in biological systems has long been established, and the current clinical unmet need is to support the clinical implications of spatial heterogeneity through experimental results and the development and integration of robust analytical, genomic, and molecular imaging modalities to address this challenge, such that we can control this heterogeneity and improve oncologic treatment outcomes in patients. The multiple complex interactions among diverse intra- and extracellular processes that lead to spatial and/or temporal heterogeneity enabling several cell phenotypes and various gene expression archetypes to emerge from the same lesion (genetic background) have been well documented in other reviews.[16−19] Here, we wanted to focus on examples of quantification of heterogeneity through two complementary recent technological advancements: (a) how intratumor heterogeneity can be assessed from clinical radiological data to provide meaningful diagnostic and therapeutic interventions and (b) how spatial transcriptomics and single-cell data can be leveraged to better identify therapeutic vulnerabilities and treatment strategies. Correlating radiological heterogeneity features to spatial transcriptomics and/or histopathology data can provide insights that may significantly improve therapeutic outcomes in patients.

■ MOLECULAR IMAGING OF INTRATUMOR HETEROGENEITY

The most commonly used clinical imaging modalities of computed tomography (CT), magnetic resonance imaging (MRI), positron emission tomography (PET), and single-photon emission computed tomography (SPECT) perform quantitative standard region of interest (ROI) analysis that generates a mean parameter for all considered voxels and therefore does not necessarily estimate underlying spatial distribution. However, sophisticated image analysis methods have been developed recently to quantify spatial heterogeneity in these same imaging data obtained from CT, MRI, and PET/SPECT images.[20] These methods can essentially add vital information about intratumor heterogeneity over assessed simple biomarkers such as tumor size and function and thus either quantify overall tumor spatial complexity or identify the tumor subregions that may drive disease transformation, progression, and drug resistance.

Histogram Analysis. Histogram analysis is the most common and popular method of characterization of intratumor heterogeneity in imaging data. It measures image heterogeneity using parameters such as standard deviation, *n*th centile, interquartile range, kurtosis, and skewness as well as mean and median value[21a,b] and calculates the pixel intensity values and displays the distribution of pixels or "local spatial image density" in a grayscale mode.

In a study by Emblem et al., the diagnostic accuracies for grading gliomas in patients were compared using the histogram analysis of normalized cerebral blood volume (cBV) maps with the hot-spot method for dynamic contrast-enhanced MRI in the patients. It was observed that the diagnostic accuracy and sensitivity of detection with histogram analysis for blood volume heterogeneity was much higher (∼90%) than that for the hot-spot method (55−76%).[22] In another study by Ma et al., the authors demonstrated the utility of the histogram method in delineating the heterogeneous morphological features of the tumor vasculature for patients with histologically confirmed glioblastoma (GBM) or lymphoma or solitary metastatic tumor. Patients underwent dynamic susceptibility contrast-enhanced MRI (DSCE-MRI) along with conventional MRI to probe the heterogeneity in tumor vasculature along with other changes in tumor anatomy. Semiquantitative histogram analysis, where six histogram parameters were analyzed from the normalized rCBV, was able to accurately distinguish different enhancing and perienhancing lesions for GBMs, lymphoma, and patients with solid metastatic lesions.[23] Since GBM pathology has well-documented demonstrations of heterogeneous morphological features of tumor capillaries with varying degrees of permeability within the same tumor, GBM images were mostly studied for identifying intratumor heterogeneity with such histogram analysis methods. In other dynamic MRI studies (DCE-MRI) for monitoring tumor response to treatment in GBM patients, Peng et al. were able to quantify, with modified full width at half-maximum (mFWHM) analysis of wash-in slope histograms, the changes in tumor heterogeneity in response to radiotherapy. Such tumor heterogeneity analysis demonstrated for brain tumors validated how tumor heterogeneity could function as an independent marker, rather than just tumor size alone, in predicting intratumor heterogeneity.[24a,b]

Texture Analysis. Tumor heterogeneity analysis as a prognostic factor can improve the grading of tumors.[25] A limitation of histogram analysis is the inability to retain the spatial arrangement of the voxels. Other mathematical models, such as texture analysis and fractal analysis, can account for intralesional heterogeneity, thus adding significant value to radiological data in patients. Texture analysis applies mathematical models and statistics-based methods to measure the exact pixel position and the relationship between neighboring pixels. For a particular lesion, texture analysis involves extraction of spatial information as gray-level intensity that ultimately generates spatial "texture features".

Texture analysis has been applied to CT and MRI images and resulted in improved tumor diagnosis. In the case of CT, unenhanced, contrast-enhanced, and derived images (such as perfusion CT) can be analyzed for heterogeneity with texture analysis. In a study by Huang et al., using statistics-based texture analysis, the authors correlated the 2D normalized autocovariance coefficient to interpixel correlations and were able to differentiate benign (84) from malignant (80) liver lesions in CT images by inferring differences in spatial textures.[26] Differentiating benign from malignant lesions and therefore improving clinical diagnosis, based on the difference in spatial heterogeneity of the lesion without the need for any external CT contrast agent, is impactful for patient outcomes as patients often display renal toxicity from the use of iodinated CT contrast agents. Another study by Ng et al. showed the CT texture analysis approach to account for spatial heterogeneity as a diagnostic biomarker in colorectal cancer patients. In this study, texture features were compared between the largest cross-sectional area and the entire tumor, and through measurements of entropy and uniformity the authors reported how the entire tumor rather than the chosen largest cross-sectional area was more representative of the tumor heterogeneity.[27] The potential of CT texture analysis in the assessment and correlation of vascular heterogeneity, which results in focal areas of hypoxia in the tumor, has been

https://doi.org/10.1021/acsomega.2c06659
ACS Omega 2023, 8, 6126−6138

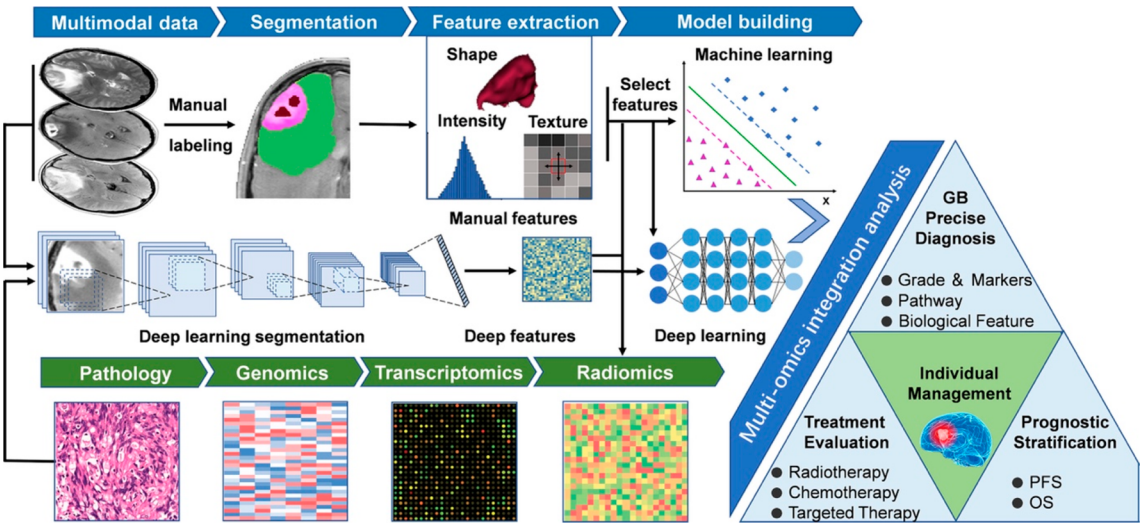

Figure 1. Neurooncology radiomics study workflow. (1) Multimodal imaging and biological data acquisition. (2) Data preprocessing and standardization. (3) Delineation of regions of interest, including manual segmentation and deep learning based segmentation. (4) Radiomics feature extraction using predefined algorithms or deep learning techniques. (5) Data analysis, feature reduction, and/or selection for further analysis of machine learning and/or deep neural networks. (6) Multiomics and clinical information integrated model training and testing, guiding individualized disease diagnosis, treatment evaluation, and prognosis prediction. GB, glioblastoma; OS, overall survival; PFS, progression free survival. Adapted from ref 24b. CC BY 4.0.

demonstrated in patients of both colorectal and primary nonsmall cell lung cancer (NSCLC).[28,29] In patients with renal lesions, again CT texture analysis was able to differentiate renal lesions with excellent sensitivity and specificity.[30]

Similarly, texture analysis of MRI data has also been applied to account for spatial heterogeneity, most significantly in breast, liver, and brain tumor studies. For example, in breast cancer, apart from being able to distinguish between just benign and malignant lesions of breast cancer, texture analysis using a co-occurrence matrix successfully differentiated invasive lobular carcinoma (ILC) from invasive ductal carcinoma (IDC), two common forms of invasive breast cancer.[31]

Apart from improved diagnosis and predicting survival outcomes in patients, texture analysis of CT images has shown the potential to assess response to therapy, although only a few studies have explored this so far. Coarse texture analysis and uniformity in texture ratios served as significant predictors of overall survival in colorectal cancer patients (receiving cytotoxic therapy) independent of the tumor stage or in renal cell cancer patients on antivascular therapy.[32,33] In fact, texture analysis proved to be a better predictor of treatment response in renal cell cancer metastases treated with tyrosine kinase inhibitors compared to the current scale of treatment assessment, which is response evaluation criteria in solid tumors (RECIST).[34] In another study of ∼200 women, Waugh et al. for the first time used CT texture analysis and mapped spatial heterogeneity from entropy-based features of the co-occurrence matrix to classify breast cancer subtypes based on pixel intensity distributions of CT images. Such a classification could potentially improve noninvasive monitoring and follow-up of breast cancer patients on different treatment regimens.[35] Interestingly, only a few studies in MRI have attempted to assess heterogeneity with treatment response.[36] However, these studies have shown encouraging results that prove that texture changes in MRI can be a potential biomarker for treatment responses, such as texture changes observed in T_1 and T_{2w} MRI of non-Hodgkin lymphoma patients at staging, followed by post first and fourth rounds of chemotherapy.[37]

Compared to CT and MRI, the potential of texture analysis in PET imaging, especially for diagnosis, has not been widely explored.[38,39] One of the reasons for this is the inherent low spatial resolution of PET images and large variability in implemented methodology.[40] However, a few attempts at texture analysis of PET images as a predictive marker of response to chemoradiation have shown that local (homogeneity, baseline entropy) and regional (size) texture parameters were better indicators than standardized uptake value (SUV) measurements in differentiating responders versus nonresponders.[41,42] Although texture analysis alone of PET data has not been useful in the assessment of spatial heterogeneity, combination of image-derived texture features from both PET and CT or PET and MRI have been able to predict lung metastases in soft tissue sarcomas and characterized renal cell carcinoma[43,44] (Figure 1).

Fractal Analysis. Fractal dimensions can be indicative of surface texture heterogeneity as well and therefore used in medical imaging where images reveal organs that have fluctuations in space and time and cannot be differentiated or characterized using only a spatial or temporal scale.[45] The most useful fractal analysis model is the fractional Brownian motion model which quantifies the intensity surface of a medical image as the end result of a random walk[46] and thereby correlates texture heterogeneity to fractal dimensions. With the use of fractal analysis, images of two textures for example can be distinguished based on the measure of lumpiness in them. As in texture-based methods, fractal analysis has been used also to distinguish as well as characterize benign and malignant lesions such as by Kido et al. where in fractal analysis of CT images benign hamartomas displayed a lower 2D fractal volume compared to malignant bronchogenic carcinomas, tuberculomas, and pneumonias.[47] Other studies utilized 3D fractal dimensions from regular CT images and were able to differentiate adenocarcinomas from squamous cell carcinomas and to correlate greater spatial heterogeneity in

https://doi.org/10.1021/acsomega.2c06659
ACS Omega 2023, 8, 6126−6138

malignant nodes of colorectal cancer versus benign nodes with an accuracy of 88%. Fractal analysis was useful in patients with colorectal cancer where both fractal dimension and abundance from CT perfusion images were higher in the cancer versus normal bowel,[48] and in repeatability measurements CT perfusion data of rectal adenocarcinoma patients, 2D and 3D fractal analysis of regional blood flow showed great correlation and good reproducibility.[49] Application of fractal geometry analysis to MRI analysis has been mostly for brain tumor MR images. For example, in a study by Di Ieva et al., patients with recurrent malignant brain tumors were imaged with MRI, where susceptibility weighted MR imaging was used to assess the changes in tumor vasculature. The qualitative heterogeneity patterns from MR images, analyzed by fractal-based analysis methods, were able to quantify the vascular heterogeneity and aided in radiology follow-up of brain tumors.[50] It was first shown by Rose et al. that spatial heterogeneity in dynamic contrast MRI (DCE-MRI) maps could be quantified also by fractal analysis and further be correlated to tumor grade.[51] In other studies, fractal analysis of voxel-based DCE-MRI data of breast cancer patients was able to deconvolute the texture at various spatial-frequency scales in a more accurate manner and therefore be a marker for early prediction in breast cancer.[52]

Texture-based and fractal-based analyses of radiological data have been also used for assisting in planning for therapy. Targeted radiation therapy is an area of cancer therapy where a statistics-based model of texture analysis on a coregistered PET/CT image in the clinic could identify abnormal nodes for radiotherapy by utilizing increased heterogeneity information in PET images and higher uniformity in CT. Tumor delineation, which is essential for oncologists before radiation therapy, was found to correlate better with automated texture-based segmentation as compared to the traditional thresholding SUV method.

Table 1 summarizes these imaging methods and the spatial heterogeneity analysis for different types of cancers.

New Imaging Methods Focusing on Spatial Heterogeneity Assessment. Metabolic activity in tumor cells is a well-established therapeutic target and a route for tumor evasion. Within the same tumor, different spatial distributions of metabolically distinct cell populations exist which are partly driven by hypoxic gradients existing within a tumor.[53−56] This distribution can be quantified based on different drug responses displayed by them with the appropriate analysis method applied to the cell-level imaging data. A new analytical method was able to distinguish cell-level spatial heterogeneity in optical metabolic imaging data (obtained from two-photon microscopy experiments) and applying density-based clustering and spatial principal component analysis (SPA) to relate the multivariate measurements of cell metabolism[57,58] with spatial trends across models and treatment conditions.[59] Briefly, the optical imaging data quantified the mean lifetimes (ζm) of NAD(P)H and FAD, which are markers for metabolically different cell populations within the same tumor[60−63] both in xenografts and in 3D organoids. Spatial patterns of cellular drug response were correlated with drug diffusion to assess the influence of drug accessibility on cellular metabolic distributions. These methods could be translated to other nonoptical metabolic imaging data acquired over an entire organoid volume or a superficial tumor volume to characterize 3D distributions of metabolism and drug response.

Table 1. Summary of Imaging Methods and the Various Analysis Methods Used for Assessment of Spatial Heterogeneity in Different Cancers

spatial heterogeneity analysis method	imaging modality	cancer type	ref
histogram analysis	CT	soft tissue sarcoma	21b
	MRI	GBM	22
	MRI	GBM	23
	MRI	GBM	24
texture analysis	CT	liver lesions	26
	CT	colorectal cancer	27, 28, 32
	CT	NSCLC	29
	CT	renal	30, 34
	CT	breast cancer	35
	MRI	breast cancer	31
	MRI	limb sarcomas	36
	MRI	non-Hodgkin lymphoma	37
	PET	sarcomas	38, 41
	PET	head and neck	42
	PET	lung metastases (soft tissue sarcomas)	43
	PET	renal cell carcinoma	44
fractal analysis	CT	bronchogenic hamartomas	47
	CT	colorectal cancer	48
	CT	rectal adenocarcinoma	49
	MRI	brain tumors	50, 51
	MRI	breast	52

Optical microscopy methods can provide rich contrast visualization of the tumor microenvironment; however, due to the limitation of low-depth penetration only a few micrometers of tissue depth can be assessed.[64] Optoacoustic/photoacoustic imaging, a relatively new technique that combines the advantage of rich optical contrast and high spatial resolution of ultrasound, can image at a larger penetration depth (approximately centimeter range) and therefore has great potential for clinical translation.[65] Li et al. recently developed a multispectral optoacoustic mesoscope (MSOM) for solid tumor imaging, a unique investigational tool for assessing the spatial heterogeneity of tumor vasculature and tumor hypoxia at resolutions much higher (~50 μm) than what is offered by the current optoacoustic systems (100−150 μm). Focal hypoxia is another prognostic biomarker of tumor progression in solid tumors; therefore, quantifying hypoxia maps in the overall tumor can provide valuable information for screening patients for personalized treatments.[66]

Yet another imaging modality that has gained momentum in the past few years for investigating the spatial distribution of a variety of molecules in the complex biological system is mass spectrometry imaging (MSI). MSI attempts to provide the relative abundance of various molecules in a spatially resolved manner without the need for histological dissection or target-specific reagents as required in histopathological examinations of entire tumor tissue. Different ionization methods (MALDI, DESI, LEASI, SIMS) can be used, resulting in ion density maps predicting the relative intensity for each m/z value detected at a particular spatial localization.[67]

Together, these newer molecular imaging methods have the potential to obtain spatially resolved data from entire tumor regions and with analysis methods such as histogram or texture- or fractal-based analysis can provide vital information

https://doi.org/10.1021/acsomega.2c06659
ACS Omega 2023, 8, 6126−6138

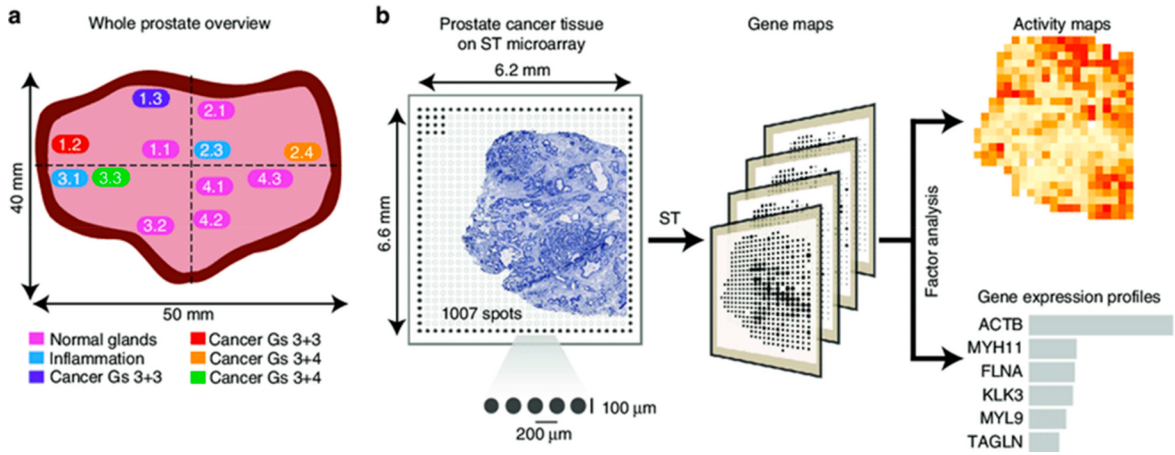

Figure 2. Spatial transcriptomics (ST) study design in prostate cancer. (a) Sample location used in this study and annotations made by a pathologist. The section annotations are color coded. Prostate size is indicated by the scale bar. (b) The 1007 spatially barcoded spots of the spatial microarray. The barcoded spots have a diameter of 100 μm and have a 200 μm center-to-center distance. Orientation and lack spatial barcodes are denoted by filled circles. The ST procedure yields matrixes with read counts for every gene in every spot, which are then decomposed by factor analysis resulting in a set of factors ("cell types"), each comprising one activity map and one expression profile. Adapted from ref 12. CC BY 4.0.

regarding the intratumor spatial heterogeneity of tumors in a noninvasive manner. In clinical diagnosis, assessment of treatment responses, grading tumors, and treatment planning, this information on intratumor heterogeneity will be of critical value in guiding clinicians and radiologists.

■ SPATIAL TRANSCRIPTOMICS IN CANCER

Genomic and transcriptomic analyses have revealed multiple mutations including driver mutations of KRAS, CDKN2A, TP53, and SMAD4.[68] Most of such characterization has been at a bulk level, with a few exceptions such as quantifying epithelial−mesenchymal heterogeneity at tumor interior versus invasive edge.[69,70] Traditional transcriptomic methods result in loss of spatial information. To address this caveat, multiple spatial transcriptomic (ST) methods have been developed recently (Figure 2).

In a study involving engrafted human pancreatic ductal adenocarcinoma (PDAC) in ischemic hind limbs of nude mice, gene expression was observed to vary spatially depending on oxygenation of the microenvironment.[71] In the control group (normoxic conditions), the subgroups (SGs) identified by spatial transcriptomics had diverse functions, such as enrichment of genes involved in proliferation in SG2, SG3, SG4, and SG11, but under hypoxic condition only SG6 showed properties of proliferation. Also, in the control group, SG10 showed enrichment of genes involved in response to hypoxia and angiogenesis, but in the hypoxic group, genes related to angiogenesis and collagen organization were enriched in SG4. Both ST and immunohistochemical (IHC) analyses revealed that lactate dehydrogenase A (LDHA) expression was found in the tumor boundary for both groups, but AKT was only upregulated in hypoxia. All subgroups under hypoxic condition showed a high metabolic rate, as revealed by GO and KEGG analysis. In another study of three PDAC human tumor samples, microarray-based ST methods were integrated with single-cell RNA-seq to determine spatial patterns of gene expression by capturing the transcriptomes of a set of adjacent cells.[72] Multimodal intersection analysis was performed to annotate the precise cellular composition of distinct tissue regions. Interestingly, different cell types—ductal cells, macrophages, dendritic cells, and cancer cells—had spatially enriched zones. Also, inflammatory fibroblasts and cancer cells that colocalized spatially exhibited stress-response profiles, thus deciphering the spatial architecture seen in PDAC.

Besides PDAC, spatial and temporal intrapatient heterogeneity of metastatic tumors has been investigated in prostate adenocarcinoma tissue.[73] Here, unbiased clustering pinpointed a subset of samples with enrichment of the small-cell neuroendocrine prostate cancer (SCNC) signature: low to absent expression of androgen receptor (AR) signaling; inactivation of TP53, PTEN, and RB1 genes; elevated expression of ASCL1 and genes associated with small cell morphology; and increased levels of E2F1 and CDKN2A, reminiscent of observations in small cell lung cancer.[74] Among 14 patients who underwent therapy, only three of them evolved to an SCNC phenotype from an adenocarcinoma phenotype, with varied levels of loss of AR signaling. Further, analysis of 176 primary and metastatic prostate tumors revealed that both phenotypes (adenocarcinoma, SCNC) could coexist for a patient in distinct metastatic lesions, thereby indicating lineage plasticity.[75] In another prostate cancer study, tissue samples from the patients who underwent radical prostatectomy were analyzed using an artificial intelligence (AI) based method.[76] Differences between multiparametric MRI (mp-MRI) invisible and mp-MRI visible prostate cancer tumors were visualized at a single-cell resolution through the annotated pipeline of segmentation, cell typing, modeling of tumor architecture and spatial interactions, and the employment of software-generated masks. The visible mp-MRI tumors did not show specific boundaries between the stromal and glandular components, but the invisible ones had a rounded glandular structure and had less closely spaced glands interspersed with stroma, thus bearing more similarity to normal prostate tissue.[76] Similarly, spatial transcriptomics on patient samples with adenocarcinoma post-radical prostatectomy revealed tissue-wide gene expression heterogeneity. An expression gradient of genes such as FOSB, AQP3, and NR4A1 was observed between the tumor and stroma.[12] A novel deconvolution approach analyzed transcriptomes of nearly 6750 tissue regions comprising stroma, normal and PIN glands, immune cells, and cancer. This method showed accuracy in delineating the extent of

https://doi.org/10.1021/acsomega.2c06659
ACS Omega 2023, 8, 6126−6138

cancer foci, similar to pathologist annotations, without directly looking at histological changes. Put together, spatial transcriptomic approaches have unraveled how different parts of a tumor may manifest the different stages of cancer progression, further indicating genetic and/or nongenetic components of cancer evolution at play, including those driven by different therapies. Further, spatial transcriptomics data can be used to develop spatially resolved metabolic network models of prostate tumor microenvironment,[77] thus identifying malignant cell-specific metabolic vulnerabilities targetable by small molecule compounds. For instance, based on the identification of spatial segregation of regions showing enrichment in fatty acid synthesis and desaturation, it was predicted that inhibiting the fatty acid desaturase SCD1 may selectively kill cancer cells. Thus, spatial transcriptomic data can also help pinpoint selective drug targets for specific cancer types.

In addition to spatial transcriptomics, digital spatial profiling (DSP) can decode the underlying heterogeneity patterns in a tumor. DSP quantifies the abundance of both RNAs and proteins in spatially distinct regions using multiplexing, which is counting the uniquely indexed oligonucleotides to specific targets of interest in a fixed tissue.[78] These oligonucleotides can be attached to antibodies or RNA probes though a linker that is photocleavable; that is, light projecting onto the tissue sample can release the photocleavable oligonucleotides in each spatial region. These light patterns can be manipulated to help profile distinct regions or cell type in a tumor or its microenvironment.[79] In a study using DSP to study samples obtained from 27 patients who died of metastatic castration resistant prostate cancer,[80] 141 regions of interest from 53 metastases (from diverse anatomic sites of tumor dissemination) were analyzed. Six phenotypes of metastatic prostate cancer were identified, based on expression levels of genes associated with androgen receptor (AR) and a small cell neuroendocrine (NE) phenotype: AR+/NE−, AR^{low}/NE−, AR−/NE−, AR−/NE^{low}, AR+/ NE+, and AR−/NE+. The DSP measurements of AR and NE activity scores—when averaged across regions of interest for a given sample—correlated well with bulk RNA-seq measurements done on corresponding frozen tumor tissue, suggesting a high level of intrapatient homogeneity. The majority of metastases were also devoid of significant inflammatory infiltrates, as they expressed at high levels B7-H3 (CD276), an immune checkpoint protein similar to PD-L1 (CD274).[81] Thus, DSP can accurately classify tumor phenotype, assess heterogeneity in tumors and stromal components, and identify aspects of tumor biology involving the immunological composition of metastases.

Beyond PDAC and prostate cancer, spatial transcriptomics has also been applied to breast cancer. Spatial mapping of samples from eight patients undergoing mastectomies revealed heterogeneity between sites based on their proximity to the tumor.[82] High copy number aberrations (CNAs) were identified at the morphologically normal epithelium sites closer to the tumor, but this variation was unable to explain diversity in corresponding gene expression profiles or mRNA abundance. Spectral coclustering was used to identify biclusters, i.e., coexpressed sets of genes that are commonly upregulated (or downregulated) in certain samples closer to the tumor than those that are further away. This comprehensive spatial CNA and mRNA characterization of morphologically normal epithelia from primary tumors of patients representing different molecular subtypes suggested that Wnt signaling may be one of the first ones to change in breast cancer progression. In another spatial transcriptomic analysis of microdissected tissues from the triple-negative breast cancer (TNBC) cell line MDA-MB-231 xenograft model, three cell-type clusters in primary tumor and axillary lymph node metastasis were revealed.[83] Two of these clusters were identified to be stem-cell-like (CD44/MYC-high, HMGA1-high). In scRNA-seq analysis on TNBC patient samples, two cancer stem-cell-like populations were detected similar to that observed in the xenograft model, highlighting potential common principles of heterogeneity in tumors. Given the complementary information available through spatial transcriptomics/digital profiling and scRNA-seq/proteomics, methods integrating insights from these can be powerful tools for potentially categorizing patients into different therapeutic regimes, depending on archetypes observed in a given tumor sample.

■ COMPUTATIONAL TOOLS FOR SPATIAL TRANSCRIPTOMICS DATA ANALYSIS

Many computational tools are being developed to integrate scRNA-seq and spatial transcriptomics. One such tool is SPOTlight;[84] it uses nonnegative matrix factorization (NMF) to obtain cell-type specific topic profiles. Its performance was tested by using synthetic mixtures comprising of two to eight cells from the peripheral blood mononuclear cell (PBMC) scRNA-seq data sets. When tested on these synthetic mixtures, it showed a sensitivity of 0.911, an accuracy of 0.78, and a median Jensen Shannon divergence (JSD) value of 0.160, thus indicating high accuracy of estimated cell type proportions. It was also able to detect in a sensitive manner different cell types and other subtle cell states at their expected spatial locations, and predict accurately despite shallower sequencing.

Another computational tool that identifies statistically significant spatial gene expression trends is Trendsceek.[85] It ranks and assesses the significance of spatial trends seen for each gene, thus identifying the set of genes for which dependencies exist between spatial distribution of cells and corresponding gene expression in those cells. It uses an approach where the spatial location of a cell is given by an assigned point, and expression levels are captured by a mark on each point. It was used to probe gene expression patterns from mouse olfactory bulb and breast tumor sections. Thus, this nonparametric method incorporates both spatial and expression-level information for a gene, thereby overcoming limitations of approaches using only one-dimensional information—pseudospace[86] or pseudotime.[87,88] Several genes implicated in breast cancer were found to have crucial spatial patterns, such as the transcription factor KLF6 and the transmembrane protein PMEPA1.

Besides the above-mentioned tools, a method designed for digital analysis of pathology whole-slide images identified the molecular traits and showed a significantly statistical connection between survival and heterogeneity.[89] Methods using a deep learning algorithm (ST-Net) that combine spatial transcriptomics and histology images to capture high-resolution expression heterogeneity have also been recently developed.[90] ST-Net was trained on spatial transcriptomic data from 68 breast tissue sections taken from 23 patients and could predict the expression of 102 genes that correlated well with experimental measurements too. It takes a 224 × 224 pixel patch of the histopathology image corresponding to approximately 150 × 150 μm^2 and predicts the expression of 250

https://doi.org/10.1021/acsomega.2c06659
ACS Omega 2023, 8, 6126−6138

specific genes. It was trained iteratively using leave-one-out analysis, i.e., taking 22 patients. Thus, its performance is affected by experimental noise in spatial transcriptomics data as well as the limited sequencing depth. For independent validation of this method, breast cancer samples from the 10x Genomics Spatial Gene Expression data set were used. Corresponding transcriptomic data set included measurements for 234 of the 250 genes that ST-Net was trained to predict. Out of the 234 genes available, the predicted expression of 207 of them were positively correlated with that seen in experimental data. Next, when applied to breast cancer samples in TCGA, ST-Net was used to scan hematoxylin and eosin (H&E) images of 1550 samples from 1093 patients without any retraining. Because TCGA only has bulk RNA-seq data, a pseudobulk expression profile for each sample was derived from ST-Net predictions. For 177 out of 250 genes whose expression ST-Net could spatially resolve and predict, the correlation with experimental measurements was positive. Further, the inferred expression levels could help distinguish histological subtypes in breast cancer infiltrating ductal adenocarcinoma and infiltrating lobular carcinoma. Finally, ST-Net could also predict the top five genes that showed the highest variation in intratumor expression—GNAS, FASN, AEBP1, SPARC and BGN. Given that heterogeneity itself, instead of mean expression levels, can be a marker of aggressiveness in breast cancer too,[91] the framework proposed by ST-Net can be helpful in identifying patients with worse prognoses across multiple cancer types.

Table 2 summarizes the different computational tools listed in this section.

INTEGRATING SINGLE-CELL MEASUREMENTS WITH SPATIAL TRANSCRIPTOMICS

Single-cell high-throughput measurements at genomic, epigenetic, metabolomic, proteomic, and chromatin levels are becoming more popular by the day,[94−96] but they often compromise on spatial and temporal information due to the tissue dissociation step. To overcome this limitation, methods such as fluorescent *in situ* sequencing (FISSEQ)[97] have been developed to show *in vivo* mRNA localization within cells. But scaling *in situ* to perform whole genome sequencing is not easy. Thus, besides array-based approaches such as high-density spatial transcriptomics (HDST), a few methods can now obtain spatial information through approaches such as computational inference, gentle tissue dissociation, and physical separation by laser microdissection.[98,99]

One of the earlier technologies that allowed visualizing over 100 transcripts per sample with single-cell resolution is single-molecule fluorescent *in situ* hybridization (smFISH).[100] It provides absolute quantification of copy number and localization of RNA molecules and can detect low copy number transcripts as well. Earlier, it was limited by the number of available fluorescent channels, but multiplexing has now enabled using a larger number of targets ($=F^n$; F = number of fluorophores, n = number of hybridization cycles). This approach is called temporal barcoding (also called sequential FISH or seqFISH) and can visualize 10000+ genes within a single cell by using specific barcodes.[101] While both FISSEQ and seqFISH can measure the expression of various genes while retaining single-cell resolution in a given field of view, they often have long acquisition times and thus assaying whole transcriptomes of single cells over large areas of interest is yet impractical.

Table 2. Summary of Tools Used to Analyze Spatial Transcriptomics Data

computational tool	function	mode of action	advantage	disadvantage	reference
SPOTlight	integrates scRNA-seq and spatial transcriptomics	nonnegative matrix factorization (NMF)	lower computation time; provides accurate predictions even when shallowly sequenced data is used; is a sensitive tool as it was able to predict even when trained using only 100 cells	the NMF method has a nonnegativity constraint; the data normalization before the analysis is not very well studied; the NMF algorithm is stochastic and complex	84, 92
Trendsceek	identifies genes that show significant trends in a spatial manner	marked point processes	can detect spatial trends by combining location and expression information; is nonparametric	has lower accuracy in calculating true positives; has lower efficiency in identifying spatially variable genes	85, 93
ST-Net	high-resolution expression heterogeneity in histology samples	deep learning algorithm	combines expression data with cell morphology; can capture intratumor heterogeneity in gene expression; automatically differentiates between normal and tumor tissue	requires large-scale transcriptomic mapping; pathological sections need to be standardized	90

https://doi.org/10.1021/acsomega.2c06659
ACS Omega 2023, 8, 6126−6138

To overcome these limitations, sci-Space was developed to provide single-cell resolution, along with determining the spatial information on a larger scale,[102] thus offering an advantage over spatial transcriptomics where each spot can still include RNA from multiple cells. It labels nuclei using unmodified DNA oligos before single-cell RNA sequencing with specific combinatorial indexing (sci-RNA-seq). This method was used to profile 14 sagittal sections derived from two embryonic day 14 (E14.0) mouse embryos (C57BL/6N) and led to approximately 120 000 spatially resolved single-cell transcriptomes. Albeit large, this number still accounts for only 2.2% of nuclei present overall. Thus, this data was integrated with a nonspatial sci-RNA-seq mouse organogenesis cell atlas data set spanning adjacent time points −E9.5 to E13.5 and cells from a developing mouse brain atlas spanning E13.5 to E14.5, thereby endorsing the ability of sci-RNA-seq in generating spatially resolved single-cell atlases of mammalian development. How this technique is applied to investigate the dynamics of tumor progression at a single-cell level remains to be demonstrated.

A similar method that integrates histological staining and spatially resolved RNA-seq data has been developed to study mammalian tissue.[103] While it can be applied to most high-quality fresh-frozen tissue types, the spatial resolution is listed currently to 100 μm. Thus, it can be potentially used for identifying heterogeneity patterns in smaller regions of interest, thus limiting the number of cells that can be investigated at a time. Another workflow that can be applied for tumor samples is XYZeq, which encodes spatial metadata at 500 μm resolution into scRNA seq libraries.[104] This method could assign transcriptomes to single cells in the case of a mixed-species experiment consisting of human (human embryonic kidney, HEK293T) and mouse (NIH 3T3) cell mixtures. Mouse tumor models were profiled using XYZeq to capture the spatially barcoded transcriptomes from tens of thousands of cells, which led to identifying a cell migration-associated transcriptomic program in tumor-associated mesenchymal stem cells (MSCs). Thus, this method could map transcriptome and spatial localization of individual cells *in situ* and can capture both spatially variable patterns of gene expression which is a function of cellular composition and heterogeneity within a cell type depending on the spatial coordinates. Given that XYZeq can be adapted to many z-layers, it could potentially facilitate a three-dimensional map of heterogeneity within a tumor too. Together, these methods could enable better understanding of how the microenvironment shapes cell identity.

■ CONCLUSION

Noninvasive molecular imaging methods such as photoacoustic and mass spectrometry imaging and advanced image analysis using texture and fractal dimensions of conventional imaging data such as those obtained from CT or MRI or from PET/CT and PET/MRI have displayed their abilities to account for spatial heterogeneity in the entire tumor or intratumor lesion heterogeneity. However, the anisotropic nature of voxels in commonly used radiological data from CT, MRI, or PET images makes it challenging for comparing the radiological images to histology data directly. When equated to histopathology and genomics data, the final in-space resolution of radiological data (200−2000 μm for preclinical and 500−5000 μm for clinical) is orders of magnitude different and thereby making it difficult for correlating spatial heterogeneity information obtained from pathology images to radiological data.[103,104] One of the current needs is therefore to integrate spatially corrected imaging data with genomics and spatial transcriptomics data and pathology biomarkers that can bypass the caveats of heterogeneity related drug resistance in tumor and poor tumor prognosis.

Additionally, parcellation techniques which refer to grouping of "similar voxels" can isolate specific tumor subregions that might share similar tumor biologies yet differ in their abilities to resist therapy or promote progression. Parcellation methods of identifying tumor subregions with spatial heterogeneity can therefore be matched to the histology of the same subregions for correlation of imaging and histological evidence of sublocal heterogeneity. The most common methods of parcellation techniques involve distinguishing based on *a priori* assumptions (threshold classification such as median apparent diffusion coefficients (ADCs) in a diffusion-weighted MRI or binary classifiers, such as K_{trans} maps from perfusion MRI graphs) or multispectral analysis (combination of multiple imaging parameters such as K_{trans} of DCE-MRI along with SUV maxima of FDG PET). Results from the parcellation-based spatial heterogeneity studies have supported the theory that analysis of tumor subregions may be more useful than accounting for average values from the entire tumor and these results when correlated or compared to spatial transcriptomics data can help better predict tumor response to therapy or sublocal tumor progression.[105−108]

Various recent technological advancements have enabled mapping the spatiotemporal heterogeneity in tumors at varying degrees of resolution as highlighted in this review. Such a deluge of information has also triggered the development of potent computational methods that can process such high-dimensional data into biologically meaningful insights, for instance, association of different localization patterns of tumor and/or stromal cell types in a tumor with patient outcomes and metabolic heterogeneity in cancer cells within the same tumor. Noninvasive imaging methods focus on the visualization and assessment of the same biomarkers, and therefore it is of the utmost importance that future steps should integrate these advancements at technological and/or conceptual levels, with the goal of achieving a predictive systems-level multiscale understanding of the dynamic tumor microenvironment and its implication in terms of patient prognosis and outcome. This understanding can empower more targeted therapeutic interventions as well as a longitudinal monitoring of variability within patient response to therapy.

■ AUTHOR INFORMATION

Corresponding Authors

Mohit Kumar Jolly − *Centre for BioSystems Science and Engineering, Indian Institute of Science (IISc), Bangalore 560012, India*; Email: mkjolly@iisc.ac.in

Sanhita Sinharay − *Centre for BioSystems Science and Engineering, Indian Institute of Science (IISc), Bangalore 560012, India*; orcid.org/0000-0001-9910-996X; Email: sanhitas@iisc.ac.in

Authors

Pooja Annasaheb Patkulkar − *Centre for BioSystems Science and Engineering, Indian Institute of Science (IISc), Bangalore 560012, India*

https://doi.org/10.1021/acsomega.2c06659
ACS Omega 2023, 8, 6126−6138

Ayalur Raghu Subbalakshmi − *Centre for BioSystems Science and Engineering, Indian Institute of Science (IISc), Bangalore 560012, India*

Complete contact information is available at:
https://pubs.acs.org/10.1021/acsomega.2c06659

Author Contributions

P.A.P. and A.R.S.: These authors contributed equally. M.K.J. and S.S. supervised and conceived the work and revised and edited the manuscript drafts; P.A.P. and A.R.S. conducted the literature review and wrote the first draft of the manuscript.

Notes

The authors declare no competing financial interest.

■ ACKNOWLEDGMENTS

M.K.J. acknowledges support by the Ramanujan Fellowship awarded by the Science and Engineering Research Board (SERB), Department of Science and Technology (DST), Government of India (SB/S2/RJN-049/2018). S.S. acknowledges support by Dr. Kiran Mazumdar-Shaw, Chairperson and Managing Director, Biocon Limited, Bangalore, for supporting the R.I. Mazumdar Young Investigator position. S.S. acknowledges support by SERB, DST, Government of India, through a SERB Power Grant (SPG/2021/002503).

■ REFERENCES

(1) Kim, J.; DeBerardinis, R. J. Mechanisms and Implications of Metabolic Heterogeneity in Cancer. *Cell Metab* **2019**, *30* (3), 434−446.

(2) Chen, F.; Ding, K.; Priedigkeit, N.; Elangovan, A.; Levine, K. M.; Carleton, N.; Savariau, L.; Atkinson, J. M.; Oesterreich, S.; Lee, A. v. Single-Cell Transcriptomic Heterogeneity in Invasive Ductal and Lobular Breast Cancer Cells. *Cancer Res.* **2021**, *81* (2), 268−281.

(3) Ramón y Cajal, S.; Sesé, M.; Capdevila, C.; Aasen, T.; de Mattos-Arruda, L.; Diaz-Cano, S. J.; Hernández-Losa, J.; Castellví, J. Clinical Implications of Intratumor Heterogeneity: Challenges and Opportunities. *J. Mol. Med. (Berl)* **2020**, *98* (2), 161.

(4) Grzywa, T. M.; Paskal, W.; Włodarski, P. K. Intratumor and Intertumor Heterogeneity in Melanoma. *Transl Oncol* **2017**, *10* (6), 956−975.

(5) Bass, A. J.; Thorsson, V.; Shmulevich, I.; Reynolds, S. M.; Miller, M.; Bernard, B.; Hinoue, T.; Laird, P. W.; Curtis, C.; Shen, H.; Weisenberger, D. J.; Schultz, N.; Shen, R.; Weinhold, N.; Kelsen, D. P.; Bowlby, R.; Chu, A.; Kasaian, K.; Mungall, A. J.; Robertson, A. G.; Sipahimalani, P.; Cherniack, A. D.; Getz, G.; Liu, Y.; Noble, M. S.; Pedamallu, C.; Sougnez, C.; Taylor-Weiner, A.; Akbani, R.; Lee, J. S.; Liu, W.; Mills, G. B.; Yang, D.; Zhang, W.; Pantazi, A.; Parfenov, M.; Gulley, M.; Piazuelo, M. B.; Schneider, B. G.; Kim, J.; Boussioutas, A.; Sheth, M.; Demchok, J. A.; Rabkin, C. S.; Willis, J. E.; Ng, S.; Garman, K.; Beer, D. G.; Pennathur, A.; Raphael, B. J.; Wu, H. T.; Odze, R.; Kim, H. K.; Bowen, J.; Leraas, K. M.; Lichtenberg, T. M.; Weaver, S.; McLellan, M.; Wiznerowicz, M.; Sakai, R.; Lawrence, M. S.; Cibulskis, K.; Lichtenstein, L.; Fisher, S.; Gabriel, S. B.; Lander, E. S.; Ding, L.; Niu, B.; Ally, A.; Balasundaram, M.; Birol, I.; Brooks, D.; Butterfield, Y. S. N.; Carlsen, R.; Chu, J.; Chuah, E.; Chun, H. J. E.; Clarke, A.; Dhalla, N.; Guin, R.; Holt, R. A.; Jones, S. J. M.; Lee, D.; Li, H. A.; Lim, E.; Ma, Y.; Marra, M. A.; Mayo, M.; Moore, R. A.; Mungall, K. L.; Nip, K. M.; Schein, J. E.; Tam, A.; Thiessen, N.; Beroukhim, R.; Carter, S. L.; Cho, J.; DiCara, D.; Frazer, S.; Gehlenborg, N.; Heiman, D. I.; Jung, J.; Kim, J.; Lin, P.; Meyerson, M.; Ojesina, A. I.; Pedamallu, C. S.; Saksena, G.; Schumacher, S. E.; Stojanov, P.; Tabak, B.; Voet, D.; Rosenberg, M.; Zack, T. I.; Zhang, H.; Zou, L.; Protopopov, A.; Santoso, N.; Lee, S.; Zhang, J.; Mahadeshwar, H. S.; Tang, J.; Ren, X.; Seth, S.; Yang, L.; Xu, A. W.; Song, X.; Xi, R.; Bristow, C. A.; Hadjipanayis, A.; Seidman, J.; Chin, L.; Park, P. J.; Kucherlapati, R.; Ling, S.; Rao, A.; Weinstein, J. N.; Kim, S. B.; Lu, Y.; Bootwalla, M. S.; Lai, P. H.; Triche, T.; van den Berg, D. J.; Baylin, S. B.; Herman, J. G.; Murray, B. A.; Askoy, B. A.; Ciriello, G.; Dresdner, G.; Gao, J.; Gross, B.; Jacobsen, A.; Lee, W.; Ramirez, R.; Sander, C.; Senbabaoglu, Y.; Sinha, R.; Sumer, S. O.; Sun, Y.; Iype, L.; Kramer, R. W.; Kreisberg, R.; Rovira, H.; Tasman, N.; Haussler, D.; Stuart, J. M.; Verhaak, R. G. W.; Leiserson, M. D. M.; Taylor, B. S.; Black, A. D.; Carney, J. A.; Gastier-Foster, J. M.; Helsel, C.; McAllister, C.; Ramirez, N. C.; Tabler, T. R.; Wise, L.; Zmuda, E.; Penny, R.; Crain, D.; Gardner, J.; Lau, K.; Curely, E.; Mallery, D.; Morris, S.; Paulauskis, J.; Shelton, T.; Shelton, C.; Sherman, M.; Benz, C.; Lee, J. H.; Fedosenko, K.; Manikhas, G.; Potapova, O.; Voronina, O.; Belyaev, D.; Dolzhansky, O.; Rathmell, W. K.; Brzezinski, J.; Ibbs, M.; Korski, K.; Kycler, W.; Łaźniak, R.; Leporowska, E.; Mackiewicz, A.; Murawa, D.; Murawa, P.; Spychała, A.; Suchorska, W. M.; Tatka, H.; Teresiak, M.; Abdel-Misih, R.; Bennett, J.; Brown, J.; Iacocca, M.; Rabeno, B.; Kwon, S. Y.; Kemkes, A.; Curley, E.; Alexopoulou, I.; Engel, J.; Bartlett, J.; Albert, M.; Park, D. Y.; Dhir, R.; Luketich, J.; Landreneau, R.; Janjigian, Y. Y.; Cho, E.; Ladanyi, M.; Tang, L.; McCall, S. J.; Park, Y. S.; Cheong, J. H.; Ajani, J.; Camargo, M. C.; Alonso, S.; Ayala, B.; Jensen, M. A.; Pihl, T.; Raman, R.; Walton, J.; Wan, Y.; Eley, G.; Shaw, K. R. M.; Tarnuzzer, R.; Wang, Z.; Yang, L.; Zenklusen, J. C.; Davidsen, T.; Hutter, C. M.; Sofia, H. J.; Burton, R.; Chudamani, S.; Liu, J. Comprehensive Molecular Characterization of Gastric Adenocarcinoma. *Nature* **2014**, *513* (7517), 202−209.

(6) Muzny, D. M.; Bainbridge, M. N.; Chang, K.; Dinh, H. H.; Drummond, J. A.; Fowler, G.; Kovar, C. L.; Lewis, L. R.; Morgan, M. B.; Newsham, I. F.; Reid, J. G.; Santibanez, J.; Shinbrot, E.; Trevino, L. R.; Wu, Y. Q.; Wang, M.; Gunaratne, P.; Donehower, L. A.; Creighton, C. J.; Wheeler, D. A.; Gibbs, R. A.; Lawrence, M. S.; Voet, D.; Jing, R.; Cibulskis, K.; Sivachenko, A.; Stojanov, P.; McKenna, A.; Lander, E. S.; Gabriel, S.; Ding, L.; Fulton, R. S.; Koboldt, D. C.; Wylie, T.; Walker, J.; Dooling, D. J.; Fulton, L.; Delehaunty, K. D.; Fronick, C. C.; Demeter, R.; Mardis, E. R.; Wilson, R. K.; Chu, A.; Chun, H. J. E.; Mungall, A. J.; Pleasance, E.; Gordon Robertson, A.; Stoll, D.; Balasundaram, M.; Birol, I.; Butterfield, Y. S. N.; Chuah, E.; Coope, R. J. N.; Dhalla, N.; Guin, R.; Hirst, C.; Hirst, M.; Holt, R. A.; Lee, D.; Li, H. I.; Mayo, M.; Moore, R. A.; Schein, J. E.; Slobodan, J. R.; Tam, A.; Thiessen, N.; Varhol, R.; Zeng, T.; Zhao, Y.; Jones, S. J. M.; Marra, M. A.; Bass, A. J.; Ramos, A. H.; Saksena, G.; Cherniack, A. D.; Schumacher, S. E.; Tabak, B.; Carter, S. L.; Pho, N. H.; Nguyen, H.; Onofrio, R. C.; Crenshaw, A.; Ardlie, K.; Beroukhim, R.; Winckler, W.; Meyerson, M.; Protopopov, A.; Hadjipanayis, A.; Lee, E.; Xi, R.; Yang, L.; Ren, X.; Sathiamoorthy, N.; Chen, P. C.; Haseley, P.; Xiao, Y.; Lee, S.; Seidman, J.; Chin, L.; Park, P. J.; Kucherlapati, R.; Todd Auman, J.; Hoadley, K. A.; Du, Y.; Wilkerson, M. D.; Shi, Y.; Liquori, C.; Meng, S.; Li, L.; Turman, Y. J.; Topal, M. D.; Tan, D.; Waring, S.; Buda, E.; Walsh, J.; Jones, C. D.; Mieczkowski, P. A.; Singh, D.; Wu, J.; Gulabani, A.; Dolina, P.; Bodenheimer, T.; Hoyle, A. P.; Simons, J. v.; Soloway, M.; Mose, L. E.; Jefferys, S. R.; Balu, S.; O'Connor, B. D.; Prins, J. F.; Chiang, D. Y.; Neil Hayes, D.; Perou, C. M.; Hinoue, T.; Weisenberger, D. J.; Maglinte, D. T.; Pan, F.; Berman, B. P.; van den Berg, D. J.; Shen, H.; Triche, T.; Baylin, S. B.; Laird, P. W.; Getz, G.; Noble, M.; Voat, D.; Gehlenborg, N.; Dicara, D.; Zhang, J.; Zhang, H.; Wu, C. J.; Liu, S. Y.; Shukla, S.; Zhou, L.; Lin, P.; Park, R. W.; Nazaire, M. D.; Robinson, J.; Thorvaldsdottir, H.; Mesirov, J.; Thorsson, V.; Reynolds, S. M.; Bernard, B.; Kreisberg, R.; Lin, J.; Iype, L.; Bressler, R.; Erkkilä, T.; Gundapuneni, M.; Liu, Y.; Norberg, A.; Robinson, T.; Yang, D.; Zhang, W.; Shmulevich, I.; de Ronde, J. J.; Schultz, N.; Cerami, E.; Ciriello, G.; Goldberg, A. P.; Gross, B.; Jacobsen, A.; Gao, J.; Kaczkowski, B.; Sinha, R.; Arman Aksoy, B.; Antipin, Y.; Reva, B.; Shen, R.; Taylor, B. S.; Ladanyi, M.; Sander, C.; Akbani, R.; Zhang, N.; Broom, B. M.; Casasent, T.; Unruh, A.; Wakefield, C.; Hamilton, S. R.; Craig Cason, R.; Baggerly, K. A.; Weinstein, J. N.; Haussler, D.; Benz, C. C.; Stuart, J. M.; Benz, S. C.; Zachary Sanborn, J.; Vaske, C. J.; Zhu, J.; Szeto, C.; Scott, G. K.; Yau, C.; Ng, S.; Goldstein, T.; Ellrott, K.; Collisson, E.; Cozen, A. E.; Zerbino, D.; Wilks, C.; Craft, B.; Spellman, P.; Penny, R.; Shelton, T.; Hatfield, M.; Morris, S.; Yena, P.; Shelton, C.; Sherman, M.; Paulauskis, J.; Gastier-Foster, J. M.; Bowen, J.; Ramirez, N. C.;

Black, A.; Pyatt, R.; Wise, L.; White, P.; Bertagnolli, M.; Brown, J.; Chan, T. A.; Chu, G. C.; Czerwinski, C.; Denstman, F.; Dhir, R.; Dörner, A.; Fuchs, C. S.; Guillem, J. G.; Iacocca, M.; Juhl, H.; Kaufman, A.; Iii, B. K.; van Le, X.; Mariano, M. C.; Medina, E. N.; Meyers, M.; Nash, G. M.; Paty, P. B.; Petrelli, N.; Rabeno, B.; Richards, W. G.; Solit, D.; Swanson, P.; Temple, L.; Tepper, J. E.; Thorp, R.; Vakiani, E.; Weiser, M. R.; Willis, J. E.; Witkin, G.; Zeng, Z.; Zinner, M. J.; Zornig, C.; Jensen, M. A.; Sfeir, R.; Kahn, A. B.; Chu, A. L.; Kothiyal, P.; Wang, Z.; Snyder, E. E.; Pontius, J.; Pihl, T. D.; Ayala, B.; Backus, M.; Walton, J.; Whitmore, J.; Baboud, J.; Berton, D. L.; Nicholls, M. C.; Srinivasan, D.; Raman, R.; Girshik, S.; Kigonya, P. A.; Alonso, S.; Sanbhadti, R. N.; Barletta, S. P.; Greene, J. M.; Pot, D. A.; Shaw, K. R. M.; Dillon, L. A. L.; Buetow, K.; Davidsen, T.; Demchok, J. A.; Eley, G.; Ferguson, M.; Fielding, P.; Schaefer, C.; Sheth, M.; Yang, L.; Guyer, M. S.; Ozenberger, B. A.; Palchik, J. D.; Peterson, J.; Sofia, H. J.; Thomson, E. Comprehensive Molecular Characterization of Human Colon and Rectal Cancer. *Nature* **2012**, *487* (7407), 330−337.

(7) Yeo, S. K.; Guan, J. L. Breast Cancer: Multiple Subtypes within a Tumor? *Trends Cancer* **2017**, *3* (11), 753−760.

(8) Yeo, S. K.; Zhu, X.; Okamoto, T.; Hao, M.; Wang, C.; Lu, P.; Lu, L. J.; Guan, J. L. Single-Cell RNA-Sequencing Reveals Distinct Patterns of Cell State Heterogeneity in Mouse Models of Breast Cancer. *Elife* **2020**, *9*, 1−24.

(9) Juiz, N.; Elkaoutari, A.; Bigonnet, M.; Gayet, O.; Roques, J.; Nicolle, R.; Iovanna, J.; Dusetti, N. Basal-like and Classical Cells Coexist in Pancreatic Cancer Revealed by Single-Cell Analysis on Biopsy-Derived Pancreatic Cancer Organoids from the Classical Subtype. *FASEB J.* **2020**, *34* (9), 12214−12228.

(10) Suda, K.; Murakami, I.; Obata, K.; Sakai, K.; Fujino, T.; Koga, T.; Ohara, S.; Hamada, A.; Soh, J.; Nishio, K.; Mitsudomi, T. Spatial Heterogeneity of Acquired Resistance Mechanisms to 1st/2nd Generation EGFR Tyrosine Kinase Inhibitors in Lung Cancer. *Lung Cancer* **2020**, *148*, 100−104.

(11) Gallaher, J. A.; Enriquez-Navas, P. M.; Luddy, K. A.; Gatenby, R. A.; Anderson, A. R. A. Spatial Heterogeneity and Evolutionary Dynamics Modulate Time to Recurrence in Continuous and Adaptive Cancer Therapies. *Cancer Res.* **2018**, *78* (8), 2127−2139.

(12) Berglund, E.; Maaskola, J.; Schultz, N.; Friedrich, S.; Marklund, M.; Bergenstråhle, J.; Tarish, F.; Tanoglidi, A.; Vickovic, S.; Larsson, L.; Salmén, F.; Ogris, C.; Wallenborg, K.; Lagergren, J.; Ståhl, P.; Sonnhammer, E.; Helleday, T.; Lundeberg, J. Spatial Maps of Prostate Cancer Transcriptomes Reveal an Unexplored Landscape of Heterogeneity. *Nat. Commun.* **2018**, *9* (1), No. 2419.

(13) Davnall, F.; Yip, C. S. P.; Ljungqvist, G.; Selmi, M.; Ng, F.; Sanghera, B.; Ganeshan, B.; Miles, K. A.; Cook, G. J.; Goh, V. Assessment of Tumor Heterogeneity: An Emerging Imaging Tool for Clinical Practice? *Insights Imaging* **2012**, *3* (6), 573−589.

(14) Choi, Y. P.; Shim, H. S.; Gao, M.-Q.; Kang, S.; Cho, N. H. Molecular Portraits of Intratumoral Heterogeneity in Human Ovarian Cancer. *Cancer Lett.* **2011**, *307* (1), 62−71.

(15) Chowdhury, R.; Ganeshan, B.; Irshad, S.; Lawler, K.; Eisenblätter, M.; Milewicz, H.; Rodriguez-Justo, M.; Miles, K.; Ellis, P.; Groves, A.; Punwani, S.; Ng, T. The Use of Molecular Imaging Combined with Genomic Techniques to Understand the Heterogeneity in Cancer Metastasis. *Br J. Radiol* **2014**, *87* (1038), 20140065.

(16) Caiado, F.; Silva-Santos, B.; Norell, H. Intra-Tumour Heterogeneity - Going beyond Genetics. *FEBS J.* **2016**, *283* (12), 2245−2258.

(17) Melo, F. D. S. E.; Vermeulen, L.; Fessler, E.; Medema, J. P. Cancer Heterogeneity—a Multifaceted View. *EMBO Rep* **2013**, *14* (8), 686−695.

(18) Giraudeau, M.; Sepp, T.; Ujvari, B.; Renaud, F.; Tasiemski, A.; Roche, B.; Capp, J.-P.; Thomas, F. Differences in Mutational Processes and Intra-Tumour Heterogeneity between Organs. *Evol Med. Public Health* **2019**, *2019* (1), 139−146.

(19) Marusyk, A.; Almendro, V.; Polyak, K. Intra-Tumour Heterogeneity: A Looking Glass for Cancer? *Nat. Rev. Cancer* **2012**, *12* (5), 323−334.

(20) Alic, L.; Niessen, W. J.; Veenland, J. F. Quantification of Heterogeneity as a Biomarker in Tumor Imaging: A Systematic Review. *PLoS One* **2014**, *9* (10), e110300.

(21) (a) Just, N. Improving Tumour Heterogeneity MRI Assessment with Histograms. *Br. J. Cancer* **2014**, *111* (12), 2205−2213. (b) Wu, G.; Xie, R.; Li, Y.; Hou, B.; Morelli, J. N.; Li, X. Histogram analysis with computed tomography angiography for discriminating soft tissue sarcoma from benign soft tissue tumor. *Medicine* **2020**, *99* (2), e18742.

(22) Emblem, K. E.; Nedregaard, B.; Nome, T.; Due-Tonnessen, P.; Hald, J. K.; Scheie, D.; Borota, O. C.; Cvancarova, M.; Bjornerud, A. Glioma Grading by Using Histogram Analysis of Blood Volume Heterogeneity from MR-Derived Cerebral Blood Volume Maps. *Radiology* **2008**, *247* (3), 808−817.

(23) Ma, J. H.; Kim, H. S.; Rim, N.-J.; Kim, S.-H.; Cho, K.-G. Differentiation among Glioblastoma Multiforme, Solitary Metastatic Tumor, and Lymphoma Using Whole-Tumor Histogram Analysis of the Normalized Cerebral Blood Volume in Enhancing and Perienhancing Lesions. *American Journal of Neuroradiology* **2010**, *31* (9), 1699−1706.

(24) (a) Peng, S.-L.; Chen, C.-F.; Liu, H.-L.; Lui, C.-C.; Huang, Y.-J.; Lee, T.-H.; Chang, C.-C.; Wang, F.-N. Analysis of Parametric Histogram from Dynamic Contrast-Enhanced MRI: Application in Evaluating Brain Tumor Response to Radiotherapy. *NMR Biomed* **2013**, *26* (4), 443−450. (b) Liu, D.; Chen, J.; Hu, X.; Yang, K.; Liu, Y.; Hu, G.; Ge, H.; Zhang, W.; Liu, H. Imaging-genomics in glioblastoma: Combining molecular and imaging signatures. *Frontiers in Oncology* **2021**, *11*, 2666.

(25) Eccles, S. A.; Welch, D. R. Metastasis: Recent Discoveries and Novel Treatment Strategies. *Lancet* **2007**, *369* (9574), 1742−1757.

(26) Huang, Y.-L.; Chen, J.-H.; Shen, W.-C. Diagnosis of Hepatic Tumors With Texture Analysis in Nonenhanced Computed Tomography Images. *Acad. Radiol* **2006**, *13* (6), 713−720.

(27) Ng, F.; Kozarski, R.; Ganeshan, B.; Goh, V. Assessment of Tumor Heterogeneity by CT Texture Analysis: Can the Largest Cross-Sectional Area Be Used as an Alternative to Whole Tumor Analysis? *Eur. J. Radiol* **2013**, *82* (2), 342−348.

(28) Ganeshan, B.; Miles, K. A. Quantifying Tumour Heterogeneity with CT. *Cancer Imaging* **2013**, *13* (1), 140−149.

(29) Ganeshan, B.; Goh, V.; Mandeville, H. C.; Ng, Q. S.; Hoskin, P. J.; Miles, K. A. Non−Small Cell Lung Cancer: Histopathologic Correlates for Texture Parameters at CT. *Radiology* **2013**, *266* (1), 326−336.

(30) Raman, S. P.; Chen, Y.; Schroeder, J. L.; Huang, P.; Fishman, E. K. CT Texture Analysis of Renal Masses. *Acad. Radiol* **2014**, *21* (12), 1587−1596.

(31) Holli, K.; Lääperi, A.-L.; Harrison, L.; Luukkaala, T.; Toivonen, T.; Ryymin, P.; Dastidar, P.; Soimakallio, S.; Eskola, H. Characterization of Breast Cancer Types by Texture Analysis of Magnetic Resonance Images. *Acad. Radiol* **2010**, *17* (2), 135−141.

(32) Miles, K. A.; Ganeshan, B.; Griffiths, M. R.; Young, R. C. D.; Chatwin, C. R. Colorectal Cancer: Texture Analysis of Portal Phase Hepatic CT Images as a Potential Marker of Survival. *Radiology* **2009**, *250* (2), 444−452.

(33) Ganeshan, B.; Panayiotou, E.; Burnand, K.; Dizdarevic, S.; Miles, K. Tumour Heterogeneity in Non-Small Cell Lung Carcinoma Assessed by CT Texture Analysis: A Potential Marker of Survival. *Eur. Radiol* **2012**, *22* (4), 796−802.

(34) Harrison, L. C.; Luukkaala, T.; Pertovaara, H.; Saarinen, T. O.; Heinonen, T. T.; Järvenpää, R.; Soimakallio, S.; Kellokumpu-Lehtinen, P.-L. I.; Eskola, H. J.; Dastidar, P. Non-Hodgkin Lymphoma Response Evaluation with MRI Texture Classification. *Journal of Experimental & Clinical Cancer Research* **2009**, *28* (1), 87.

(35) Waugh, S. A.; Purdie, C. A.; Jordan, L. B.; Vinnicombe, S.; Lerski, R. A.; Martin, P.; Thompson, A. M. Magnetic Resonance Imaging Texture Analysis Classification of Primary Breast Cancer. *Eur. Radiol* **2016**, *26* (2), 322−330.

(36) Alic, L.; van Vliet, M.; van Dijke, C. F.; Eggermont, A. M. M.; Veenland, J. F.; Niessen, W. J. Heterogeneity in DCE-MRI Parametric

Maps: A Biomarker for Treatment Response? *Phys. Med. Biol.* **2011**, *56* (6), 1601−1616.
(37) Harrison, L. C.; Luukkaala, T.; Pertovaara, H.; Saarinen, T. O.; Heinonen, T. T.; Järvenpää, R.; Soimakallio, S.; Kellokumpu-Lehtinen, P.-L. I.; Eskola, H. J.; Dastidar, P. Non-Hodgkin Lymphoma Response Evaluation with MRI Texture Classification. *Journal of Experimental & Clinical Cancer Research* **2009**, *28* (1), 87.
(38) Eary, J. F.; O'Sullivan, F.; O'Sullivan, J.; Conrad, E. U. Spatial Heterogeneity in Sarcoma ^{18}F-FDG Uptake as a Predictor of Patient Outcome. *J. Nucl. Med.* **2008**, *49* (12), 1973−1979.
(39) Deleu, A.-L.; Sathekge, M. J.; Maes, A.; de Spiegeleer, B.; Sathekge, M.; van de Wiele, C. Characterization of FDG PET Images Using Texture Analysis in Tumors of the Gastro-Intestinal Tract: A Review. *Biomedicines* **2020**, *8* (9), 304.
(40) Hatt, M.; Tixier, F.; Pierce, L.; Kinahan, P. E.; le Rest, C. C.; Visvikis, D. Characterization of PET/CT Images Using Texture Analysis: The Past, the Present··· Any Future? *Eur. J. Nucl. Med. Mol. Imaging* **2017**, *44* (1), 151−165.
(41) O'Sullivan, F. Incorporation of Tumor Shape into an Assessment of Spatial Heterogeneity for Human Sarcomas Imaged with FDG-PET. *Biostatistics* **2005**, *6* (2), 293−301.
(42) Huan, Yu; Caldwell, C.; Mah, K.; Mozeg, D. Coregistered FDG PET/CT-Based Textural Characterization of Head and Neck Cancer for Radiation Treatment Planning. *IEEE Trans Med. Imaging* **2009**, *28* (3), 374−383.
(43) Vallières, M.; Freeman, C. R.; Skamene, S. R.; el Naqa, I. A Radiomics Model from Joint FDG-PET and MRI Texture Features for the Prediction of Lung Metastases in Soft-Tissue Sarcomas of the Extremities. *Phys. Med. Biol.* **2015**, *60* (14), 5471−5496.
(44) Antunes, J.; Viswanath, S.; Rusu, M.; Valls, L.; Hoimes, C.; Avril, N.; Madabhushi, A. Radiomics Analysis on FLT-PET/MRI for Characterization of Early Treatment Response in Renal Cell Carcinoma: A Proof-of-Concept Study. *Transl Oncol* **2016**, *9* (2), 155−162.
(45) Kuikka, J. T. Fractal Analysis in Medical Imaging. *International Journal of Nonlinear Sciences and Numerical Simulation* **2002**, DOI: 10.1515/IJNSNS.2002.3.2.81.
(46) Chen, C.-C.; DaPonte, J. S.; Fox, M. D. Fractal Feature Analysis and Classification in Medical Imaging. *IEEE Trans Med. Imaging* **1989**, *8* (2), 133−142.
(47) Kido, S.; Kuriyama, K.; Higashiyama, M.; Kasugai, T.; Kuroda, C. Fractal Analysis of Internal and Peripheral Textures of Small Peripheral Bronchogenic Carcinomas in Thin-Section Computed Tomography: Comparison of Bronchioloalveolar Cell Carcinomas With Nonbronchioloalveolar Cell Carcinomas. *J. Comput. Assist Tomogr* **2003**, *27* (1), 56−61.
(48) Goh, V.; Sanghera, B.; Wellsted, D. M.; Sundin, J.; Halligan, S. Assessment of the Spatial Pattern of Colorectal Tumour Perfusion Estimated at Perfusion CT Using Two-Dimensional Fractal Analysis. *Eur. Radiol* **2009**, *19* (6), 1358−1365.
(49) Sanghera, B.; Banerjee, D.; Khan, A.; Simcock, I.; Stirling, J. J.; Glynne-Jones, R.; Goh, V. Reproducibility of 2D and 3D Fractal Analysis Techniques for the Assessment of Spatial Heterogeneity of Regional Blood Flow in Rectal Cancer. *Radiology* **2012**, *263* (3), 865−873.
(50) Di Ieva, A.; Matula, C.; Grizzi, F.; Grabner, G.; Trattnig, S.; Tschabitscher, M. Fractal Analysis of the Susceptibility Weighted Imaging Patterns in Malignant Brain Tumors During Antiangiogenic Treatment: Technical Report on Four Cases Serially Imaged by 7 T Magnetic Resonance During a Period of Four Weeks. *World Neurosurg.* **2012**, *77* (5−6), 785.e11−785.e21.
(51) Rose, C. J.; Mills, S. J.; O'Connor, J. P. B.; Buonaccorsi, G. A.; Roberts, C.; Watson, Y.; Cheung, S.; Zhao, S.; Whitcher, B.; Jackson, A.; Parker, G. J. M. Quantifying Spatial Heterogeneity in Dynamic Contrast-Enhanced MRI Parameter Maps. *Magn Reson Med.* **2009**, *62* (2), 488−499.
(52) Machireddy, A.; Thibault, G.; Tudorica, A.; Afzal, A.; Mishal, M.; Kemmer, K.; Naik, A.; Troxell, M.; Goranson, E.; Oh, K.; Roy, N.; Jafarian, N.; Holtorf, M.; Huang, W.; Song, X. Early Prediction of Breast Cancer Therapy Response Using Multiresolution Fractal Analysis of DCE-MRI Parametric Maps. *Tomography* **2019**, *5* (1), 90−98.
(53) Heaster, T. M.; Landman, B. A.; Skala, M. C. Quantitative Spatial Analysis of Metabolic Heterogeneity Across in Vivo and in Vitro Tumor Models. *Front. Oncol.* **2019**, *9*, 1144.
(54) Carmona-Fontaine, C.; Deforet, M.; Akkari, L.; Thompson, C. B.; Joyce, J. A.; Xavier, J. B. Metabolic Origins of Spatial Organization in the Tumor Microenvironment. *Proc. Natl. Acad. Sci. U. S. A.* **2017**, *114* (11), 2934−2939.
(55) Serganova, I.; Doubrovin, M.; Vider, J.; Ponomarev, V.; Soghomonyan, S.; Beresten, T.; Ageyeva, L.; Serganov, A.; Cai, S.; Balatoni, J.; Blasberg, R.; Gelovani, J. Molecular Imaging of Temporal Dynamics and Spatial Heterogeneity of Hypoxia-Inducible Factor-1 Signal Transduction Activity in Tumors in Living Mice. *Cancer Res.* **2004**, *64* (17), 6101−6108.
(56) Saxena, K.; Jolly, M. K. Acute vs. Chronic vs. Cyclic Hypoxia: Their Differential Dynamics, Molecular Mechanisms, and Effects on Tumor Progression. *Biomolecules* **2019**, *9*, 339.
(57) Walsh, A. J.; Skala, M. C. Optical Metabolic Imaging Quantifies Heterogeneous Cell Populations. *Biomed Opt Express* **2015**, *6* (2), 559.
(58) de Back, W.; Zerjatke, T.; Roeder, I. *Statistical and Mathematical Modeling of Spatiotemporal Dynamics of Stem Cells* **2019**, *2017*, 219−243.
(59) Heaster, T. M.; Landman, B. A.; Skala, M. C. Quantitative Spatial Analysis of Metabolic Heterogeneity Across in Vivo and in Vitro Tumor Models. *Front. Oncol.* **2019**, DOI: 10.3389/fonc.2019.01144.
(60) Walsh, A. J.; Cook, R. S.; Manning, H. C.; Hicks, D. J.; Lafontant, A.; Arteaga, C. L.; Skala, M. C. Optical Metabolic Imaging Identifies Glycolytic Levels, Subtypes, and Early-Treatment Response in Breast Cancer. *Cancer Res.* **2013**, *73* (20), 6164−6174.
(61) Georgakoudi, I.; Quinn, K. P. Optical Imaging Using Endogenous Contrast to Assess Metabolic State. *Annu. Rev. Biomed Eng.* **2012**, *14* (1), 351−367.
(62) Sharick, J. T.; Favreau, P. F.; Gillette, A. A.; Sdao, S. M.; Merrins, M. J.; Skala, M. C. Protein-Bound NAD(P)H Lifetime Is Sensitive to Multiple Fates of Glucose Carbon. *Sci. Rep* **2018**, *8* (1), 5456.
(63) Liu, Z.; Pouli, D.; Alonzo, C. A.; Varone, A.; Karaliota, S.; Quinn, K. P.; Münger, K.; Karalis, K. P.; Georgakoudi, I. Mapping Metabolic Changes by Noninvasive, Multiparametric, High-Resolution Imaging Using Endogenous Contrast. *Sci. Adv.* **2018**, DOI: 10.1126/sciadv.aap9302.
(64) Garvalov, B. K.; Ertürk, A. Seeing Whole-Tumour Heterogeneity. *Nat. Biomed Eng.* **2017**, *1* (10), 772−774.
(65) Herzog, E.; Taruttis, A.; Beziere, N.; Lutich, A. A.; Razansky, D.; Ntziachristos, V. Optical Imaging of Cancer Heterogeneity with Multispectral Optoacoustic Tomography. *Radiology* **2012**, *263* (2), 461−468.
(66) Li, J.; Chekkoury, A.; Prakash, J.; Glasl, S.; Vetschera, P.; Koberstein-Schwarz, B.; Olefir, I.; Gujrati, V.; Omar, M.; Ntziachristos, V. Spatial Heterogeneity of Oxygenation and Haemodynamics in Breast Cancer Resolved in Vivo by Conical Multispectral Optoacoustic Mesoscopy. *Light Sci. Appl.* **2020**, *9* (1), 57.
(67) Porta Siegel, T.; Hamm, G.; Bunch, J.; Cappell, J.; Fletcher, J. S.; Schwamborn, K. Mass Spectrometry Imaging and Integration with Other Imaging Modalities for Greater Molecular Understanding of Biological Tissues. *Mol. Imaging Biol.* **2018**, *20* (6), 888−901.
(68) Morjaria, S.; Morjaria, S. Driver Mutations in Oncogenesis. *International Journal of Molecular & Immuno Oncology* **2021**, *6* (2), 100−102.
(69) Liu, S.; Cong, Y.; Wang, D.; Sun, Y.; Deng, L.; Liu, Y.; Martin-Trevino, R.; Shang, L.; McDermott, S. P.; Landis, M. D.; Hong, S.; Adams, A.; D'Angelo, R.; Ginestier, C.; Charafe-Jauffret, E.; Clouthier, S. G.; Birnbaum, D.; Wong, S. T.; Zhan, M.; Chang, J. C.; Wicha, M. S. Breast Cancer Stem Cells Transition between Epithelial and

Mesenchymal States Reflective of Their Normal Counterparts. *Stem Cell Reports* **2014**, *2* (1), 78−91.
(70) Brabletz, T.; Jung, A.; Reu, S.; Porzner, M.; Hlubek, F.; Kunz-Schughart, L. A.; Knuechel, R.; Kirchner, T. Variable β-Catenin Expression in Colorectal Cancers Indicates Tumor Progression Driven by the Tumor Environment. *Proc. Natl. Acad. Sci. U. S. A.* **2001**, *98* (18), 10356−10361.
(71) Sun, H.; Zhang, D.; Huang, C.; Guo, Y.; Yang, Z.; Yao, N.; Dong, X.; Cheng, R.; Zhao, N.; Meng, J.; Sun, B.; Hao, J. Hypoxic Microenvironment Induced Spatial Transcriptome Changes in Pancreatic Cancer. *Cancer Biol. Med.* **2021**, *18* (2), 616−630.
(72) Moncada, R.; Barkley, D.; Wagner, F.; Chiodin, M.; Devlin, J. C.; Baron, M.; Hajdu, C. H.; Simeone, D. M.; Yanai, I. Integrating Microarray-Based Spatial Transcriptomics and Single-Cell RNA-Seq Reveals Tissue Architecture in Pancreatic Ductal Adenocarcinomas. *Nat. Biotechnol.* **2020**, *38* (3), 333−342.
(73) Aggarwal, R. R.; Quigley, D. A.; Huang, J.; Zhang, L.; Beer, T. M.; Rettig, M. B.; Reiter, R. E.; Gleave, M. E.; Thomas, G. V.; Foye, A.; Playdle, D.; Lloyd, P.; Chi, K. N.; Evans, C. P.; Lara, P. N.; Feng, F. Y.; Alumkal, J. J.; Small, E. J. Whole Genome and Transcriptional Analysis of Treatment-Emergent Small Cell Neuroendocrine Prostate Cancer Demonstrates Intra-Class Heterogeneity. *Mol. Cancer Res.* **2019**, *17* (6), 1235.
(74) Chauhan, L.; Ram, U.; Hari, K.; Jolly, M. K. Topological Signatures in Regulatory Network Enable Phenotypic Heterogeneity in Small Cell Lung Cancer. *Elife* **2021**, *10*, e64522.
(75) Thankamony, A. P.; Subbalakshmi, A. R.; Jolly, M. K.; Nair, R. Lineage Plasticity in Cancer: The Tale of a Skin-Walker. *Cancers (Basel)* **2021**, *13* (14), 3602.
(76) Pachynski, R. K.; Kim, E. H.; Miheecheva, N.; Kotlov, N.; Ramachandran, A.; Postovalova, E.; Galkin, I.; Svekolkin, V.; Lyu, Y.; Zou, Q.; Cao, D.; Gaut, J.; Ippolito, J. E.; Bagaev, A.; Bruttan, M.; Gancharova, O.; Nomie, K.; Tsiper, M.; Andriole, G. L.; Ataullakhanov, R.; Hsieh, J. J. Single-Cell Spatial Proteomic Revelations on the Multiparametric MRI Heterogeneity of Clinically Significant Prostate Cancer. *Clin. Cancer Res.* **2021**, *27* (12), 3478−3490.
(77) Wang, Y.; Ma, S.; Ruzzo, W. L. Spatial Modeling of Prostate Cancer Metabolic Gene Expression Reveals Extensive Heterogeneity and Selective Vulnerabilities. *Sci. Rep.* **2020**, DOI: 10.1038/s41598-020-60384-w.
(78) Merritt, C. R.; Ong, G. T.; Church, S. E.; Barker, K.; Danaher, P.; Geiss, G.; Hoang, M.; Jung, J.; Liang, Y.; McKay-Fleisch, J.; Nguyen, K.; Norgaard, Z.; Sorg, K.; Sprague, I.; Warren, C.; Warren, S.; Webster, P. J.; Zhou, Z.; Zollinger, D. R.; Dunaway, D. L.; Mills, G. B.; Beechem, J. M. Multiplex Digital Spatial Profiling of Proteins and RNA in Fixed Tissue. *Nature Biotechnology 2020 38:5* **2020**, *38* (5), 586−599.
(79) Beechem, J. M. High-Plex Spatially Resolved RNA and Protein Detection Using Digital Spatial Profiling: A Technology Designed for Immuno-Oncology Biomarker Discovery and Translational Research. *Methods Mol. Biol.* **2020**, *2055*, 563−583.
(80) Brady, L.; Kriner, M.; Coleman, I.; Morrissey, C.; Roudier, M.; True, L. D.; Gulati, R.; Plymate, S. R.; Zhou, Z.; Birditt, B.; Meredith, R.; Geiss, G.; Hoang, M.; Beechem, J.; Nelson, P. S. Inter- and Intra-Tumor Heterogeneity of Metastatic Prostate Cancer Determined by Digital Spatial Gene Expression Profiling. *Nat. Commun.* **2021**, DOI: 10.1038/s41467-021-21615-4.
(81) Chakraborty, P.; Chen, E. L.; McMullen, I.; Armstrong, A. J.; Kumar Jolly, M.; Somarelli, J. A. Analysis of Immune Subtypes across the Epithelial-Mesenchymal Plasticity Spectrum. *Comput. Struct Biotechnol J.* **2021**, *19*, 3842−3851.
(82) Abdalla, M.; Tran-Thanh, D.; Moreno, J.; Iakovlev, V.; Nair, R.; Kanwar, N.; Abdalla, M.; Lee, J. P. Y.; Kwan, J. Y. Y.; Cawthorn, T. R.; Warren, K.; Arneson, N.; Wang, D. Y.; Fox, N. S.; Youngson, B. J.; Miller, N. A.; Easson, A. M.; McCready, D.; Leong, W. L.; Boutros, P. C.; Done, S. J. Mapping Genomic and Transcriptomic Alterations Spatially in Epithelial Cells Adjacent to Human Breast Carcinoma. *Nat. Commun.* **2017**, DOI: 10.1038/s41467-017-01357-y.
(83) Nakayama, J.; Matsunaga, H.; Arikawa, K.; Yoda, T.; Hosokawa, M.; Takeyama, H.; Yamamoto, Y.; Semba, K. Identification of Two Cancer Stem Cell-like Populations in Triple-Negative Breast Cancer Xenografts. *Dis. Models Mech.* **2022**, *15* (6), dmm049538.
(84) Elosua-Bayes, M.; Nieto, P.; Mereu, E.; Gut, I.; Heyn, H. SPOTlight: Seeded NMF Regression to Deconvolute Spatial Transcriptomics Spots with Single-Cell Transcriptomes. *Nucleic Acids Res.* **2021**, *49* (9), e50.
(85) Edsgärd, D.; Johnsson, P.; Sandberg, R. Identification of Spatial Expression Trends in Single-Cell Gene Expression Data. *Nat. Methods* **2018**, *15* (5), 339−342.
(86) Joost, S.; Zeisel, A.; Jacob, T.; Sun, X.; La Manno, G.; Lönnerberg, P.; Linnarsson, S.; Kasper, M. Single-Cell Transcriptomics Reveals That Differentiation and Spatial Signatures Shape Epidermal and Hair Follicle Heterogeneity. *Cell Syst* **2016**, *3* (3), 221−237.e9.
(87) Sahoo, S.; Nayak, S. P.; Hari, K.; Mandal, S.; Kishore, A.; Levine, H.; Jolly, M. K.; Purkait, P. Immunosuppressive Traits of the Hybrid Epithelial/Mesenchymal Phenotype. *Front. Immunol.* **2021**, *12*, 797261.
(88) Petropoulos, S.; Edsgärd, D.; Reinius, B.; Deng, Q.; Panula, S. P.; Codeluppi, S.; Plaza Reyes, A.; Linnarsson, S.; Sandberg, R.; Lanner, F. Single-Cell RNA-Seq Reveals Lineage and X Chromosome Dynamics in Human Preimplantation Embryos. *Cell* **2016**, *165* (4), 1012.
(89) Levy-Jurgenson, A.; Tekpli, X.; Kristensen, V. N.; Yakhini, Z. Spatial Transcriptomics Inferred from Pathology Whole-Slide Images Links Tumor Heterogeneity to Survival in Breast and Lung Cancer. *Sci. Rep.* **2020**, DOI: 10.1038/s41598-020-75708-z.
(90) He, B.; Bergenstråhle, L.; Stenbeck, L.; Abid, A.; Andersson, A.; Borg, Å.; Maaskola, J.; Lundeberg, J.; Zou, J. Integrating Spatial Gene Expression and Breast Tumour Morphology via Deep Learning. *Nat. Biomed Eng.* **2020**, *4* (8), 827−834.
(91) Chakraborty, P.; George, J. T.; Woodward, W. A.; Levine, H.; Jolly, M. K. Gene Expression Profiles of Inflammatory Breast Cancer Reveal High Heterogeneity across the Epithelial-Hybrid-Mesenchymal Spectrum. *Transl. Oncol.* **2021**, *14* (4), 101026.
(92) Devarajan, K. Nonnegative Matrix Factorization: An Analytical and Interpretive Tool in Computational Biology. *PLoS Comput. Biol.* **2008**, *4* (7), e1000029.
(93) Charitakis, N.; Ramialison, M.; Nim, H. T. Comparative Analysis of Packages and Algorithms for the Analysis of Spatially Resolved Transcriptomics Data. In *Transcriptomics in Health and Disease*; Passos, G. A., Ed.; Springer: Cham, Switzerland, 2022; pp 165−186. DOI: 10.1007/978-3-030-87821-4_7.
(94) Ahl, P. J.; Hopkins, R. A.; Xiang, W. W.; Au, B.; Kaliaperumal, N.; Fairhurst, A. M.; Connolly, J. E. Met-Flow, a Strategy for Single-Cell Metabolic Analysis Highlights Dynamic Changes in Immune Subpopulations. *Communications Biology 2020 3:1* **2020**, *3* (1), 1−15.
(95) Clark, S. J.; Lee, H. J.; Smallwood, S. A.; Kelsey, G.; Reik, W. Single-Cell Epigenomics: Powerful New Methods for Understanding Gene Regulation and Cell Identity. *Genome Biol.* **2016**, *17* (1), 72.
(96) Petelski, A. A.; Emmott, E.; Leduc, A.; Huffman, R. G.; Specht, H.; Perlman, D. H.; Slavov, N. Multiplexed Single-Cell Proteomics Using SCoPE2. *Nat. Protoc* **2021**, *16* (12), 5398−5425.
(97) Lee, J. H.; Daugharthy, E. R.; Scheiman, J.; Kalhor, R.; Yang, J. L.; Ferrante, T. C.; Terry, R.; Jeanty, S. S. F.; Li, C.; Amamoto, R.; Peters, D. T.; Turczyk, B. M.; Marblestone, A. H.; Inverso, S. A.; Bernard, A.; Mali, P.; Rios, X.; Aach, J.; Church, G. M. Highly Multiplexed Subcellular RNA Sequencing in Situ. *Science* **2014**, *343* (6177), 1360−1363.
(98) Savulescu, A. F.; Jacobs, C.; Negishi, Y.; Davignon, L.; Mhlanga, M. M. Pinpointing Cell Identity in Time and Space. *Front. Mol. Biosci.* **2020**, DOI: 10.3389/fmolb.2020.00209.
(99) Wang, N.; Li, X.; Wang, R.; Ding, Z. Spatial Transcriptomics and Proteomics Technologies for Deconvoluting the Tumor Microenvironment. *Biotechnol J.* **2021**, *16* (9), 2100041.

(100) Raj, A.; van den Bogaard, P.; Rifkin, S. A.; van Oudenaarden, A.; Tyagi, S. Imaging Individual MRNA Molecules Using Multiple Singly Labeled Probes. *Nat. Methods* **2008**, *5* (10), 877−879.
(101) Bingham, G. C.; Lee, F.; Naba, A.; Barker, T. H. Spatial-Omics: Novel Approaches to Probe Cell Heterogeneity and Extracellular Matrix Biology. *Matrix Biology* **2020**, *91−92*, 152−166.
(102) Srivatsan, S. R.; Regier, M. C.; Barkan, E.; Franks, J. M.; Packer, J. S.; Grosjean, P.; Duran, M.; Saxton, S.; Ladd, J. J.; Spielmann, M.; Lois, C.; Lampe, P. D.; Shendure, J.; Stevens, K. R.; Trapnell, C. Embryo-Scale, Single-Cell Spatial Transcriptomics. *Science (1979)* **2021**, *373* (6550), 111−117.
(103) Zhu, Q.; Shah, S.; Dries, R.; Cai, L.; Yuan, G.-C. Identification of Spatially Associated Subpopulations by Combining ScRNAseq and Sequential Fluorescence in Situ Hybridization Data. *Nat. Biotechnol.* **2018**, *36* (12), 1183−1190.
(104) Tasic, B.; Menon, V.; Nguyen, T. N.; Kim, T. K.; Jarsky, T.; Yao, Z.; Levi, B.; Gray, L. T.; Sorensen, S. A.; Dolbeare, T.; Bertagnolli, D.; Goldy, J.; Shapovalova, N.; Parry, S.; Lee, C.; Smith, K.; Bernard, A.; Madisen, L.; Sunkin, S. M.; Hawrylycz, M.; Koch, C.; Zeng, H. Adult Mouse Cortical Cell Taxonomy Revealed by Single Cell Transcriptomics. *Nat. Neurosci* **2016**, *19* (2), 335−346.
(105) O'Connor, J. P. B.; Carano, R. A. D.; Clamp, A. R.; Ross, J.; Ho, C. C. K.; Jackson, A.; Parker, G. J. M.; Rose, C. J.; Peale, F. v.; Friesenhahn, M.; Mitchell, C. L.; Watson, Y.; Roberts, C.; Hope, L.; Cheung, S.; Reslan, H. B.; Go, M. A. T.; Pacheco, G. J.; Wu, X.; Cao, T. C.; Ross, S.; Buonaccorsi, G. A.; Davies, K.; Hasan, J.; Thornton, P.; del Puerto, O.; Ferrara, N.; van Bruggen, N.; Jayson, G. C. Quantifying Antivascular Effects of Monoclonal Antibodies to Vascular Endothelial Growth Factor: Insights from Imaging. *Clin. Cancer Res.* **2009**, *15* (21), 6674−6682.
(106) Messiou, C.; Orton, M.; Ang, J. E.; Collins, D. J.; Morgan, V. A.; Mears, D.; Castellano, I.; Papadatos-Pastos, D.; Brunetto, A.; Tunariu, N.; Mann, H.; Tessier, J.; Young, H.; Ghiorghiu, D.; Marley, S.; Kaye, S. B.; deBono, J. S.; Leach, M. O.; deSouza, N. M. Advanced Solid Tumors Treated with Cediranib: Comparison of Dynamic Contrast-Enhanced MR Imaging and CT as Markers of Vascular Activity. *Radiology* **2012**, *265* (2), 426−436.
(107) Jackson, A.; O'Connor, J. P. B.; Parker, G. J. M.; Jayson, G. C. Imaging Tumor Vascular Heterogeneity and Angiogenesis Using Dynamic Contrast-Enhanced Magnetic Resonance Imaging. *Clin. Cancer Res.* **2007**, *13* (12), 3449−3459.
(108) Berry, L. R.; Barck, K. H.; Go, M. A.; Ross, J.; Wu, X.; Williams, S. P.; Gogineni, A.; Cole, M. J.; Van Bruggen, N.; Fuh, G.; Peale, F.; Ferrara, N.; Ross, S.; Schwall, R. H.; Carano, R. A. D. Quantification of Viable Tumor Microvascular Characteristics by Multispectral Analysis. *Magn. Reson. Med.* **2008**, *60* (1), 64−72.

https://doi.org/10.1021/acsomega.2c06659
ACS Omega 2023, 8, 6126−6138